Strain-driven light-polarization switching in deep ultraviolet nitride emitters

T. K. Sharma,[*,†] D. Naveh, and E. Towe[‡]
Department of Electrical and Computer Engineering, Carnegie Mellon University, 5000 Forbes Avenue, Pittsburgh, Pennsylvania 15213, USA
(Received 7 January 2011; revised manuscript received 29 May 2011; published 20 July 2011)

Residual strain plays a critical role in determining the crystalline quality of nitride epitaxial layers and in modifying their band structure; this often leads to several interesting physical phenomena. It is found, for example, that compressive strain in $Al_xGa_{1-x}N$ layers grown on $Al_yGa_{1-y}N$ ($x < y$) templates results in an anticrossing of the valence bands at considerably much higher Al composition than expected. This happens even in the presence of large and negative crystal field splitting energy in the $Al_xGa_{1-x}N$ layers. A judicious magnitude of the compressive strain can support vertical light emission (out of the c-plane) from $Al_xGa_{1-x}N$ quantum wells up to $x \approx 0.80$, which is desirable for the development of deep ultraviolet light-emitting diodes designed to operate at or below 250 nm with transverse electric polarization characteristics.

DOI: 10.1103/PhysRevB.84.035305 PACS number(s): 78.66.Fd, 78.66.Bz, 78.67.De, 68.60.Bs

I. INTRODUCTION

Deep ultraviolet (UV) nitride emitters have recently attracted a great deal of attention because of the possibility of developing more efficient, portable, and safer light sources as alternatives to conventional excimer and mercury lamps.[1–6] However, a major obstacle has been the extremely low external quantum efficiency (EQE) of the nitride emitters. A significant drop in EQE is usually observed as emission wavelengths approach the deep UV regime.[5] The EQE for light-emitting diodes (LEDs) is defined as a product of the internal quantum efficiency (IQE), carrier injection efficiency (CIE), and light extraction efficiency (LEE).[1,3–5] The internal quantum efficiency of a light emitter is related to the crystalline quality of the epitaxial layers, where a large number of defects and dislocations can lead to inferior device characteristics.[5,7] Furthermore, inadequate carrier density in p-type AlGaN barrier layers, and inappropriate band discontinuities at key heterojunction interfaces are considered to be the major factors that affect carrier injection efficiency.[3–5,7] There are ongoing efforts to improve both the IQE and the CIE by various approaches. For example, an output power of 5 (100) mW has been demonstrated under electrical (electron beam) injection for devices operating at ∼250 nm.[1,3] Similarly, low values of LEE (<8%) are reported due to absorption of the UV light at the p-side electrode.[3] Furthermore, it is now well understood that light emitted from Al-rich AlGaN layers grown on c-plane sapphire is predominantly polarized along the c-axis; this makes light extraction from LEDs a formidable task.[8–10] Several strategies, such as interconnected microdisk LED architectures and two-dimensional photonic crystal designs, have been suggested to enhance the light extraction efficiency of deep UV LEDs.[11,12]

Nevertheless, a fundamental issue has been intriguing researchers in the nitride community. It is found that light emitted by AlGaN epitaxial layers switches its polarization characteristics from transverse electric (TE) to transverse magnetic (TM) mode at some critical aluminum composition. Nam *et al.*,[8] for example, have reported that the emitted light from $Al_xGa_{1-x}N$ structures grown on c-plane sapphire switches its polarization from TE to TM mode for $x > 0.25$. Similarly, Hazu *et al.*[13] have reported polarization switching for Al content between $x = 0.25$ and $x = 0.32$ in $Al_xGa_{1-x}N$ epilayers on m-plane GaN substrates. In yet another paper, Kawanishi *et al.*[10] reported polarization switching at $x \approx 0.36$–0.41 in $Al_xGa_{1-x}N$ quantum wells on AlN/SiC templates. On the other hand, Ikeda *et al.*[14] reported polarization switching in $Al_xGa_{1-x}N$ epilayers on GaN/sapphire templates—however, at the much lower value of $x = 0.125$. They argued that although the polarization switching should have been observed at $x = 0.032$ for unstrained $Al_xGa_{1-x}N$ epilayers, it was observed at higher Al content because of finite residual strain in the AlGaN epilayers. Recently, a similar argument was invoked by Banal *et al.*[2] to explain the polarization properties of light emitted by $Al_xGa_{1-x}N$/AlN quantum well (QW) structures grown on AlN/sapphire templates; in this case, the polarization switching was observed at $x \sim 0.80$. Using a qualitative model, they were able to explain some of their data. However, an ambiguity still exists on the critical value of Al composition in the $Al_xGa_{1-x}N$ epilayers where one expects to observe the light-polarization switching behavior. More recently, Hirayama *et al.*[3] have reported they were able to observe vertical emission of light (out of the c-plane) up to $x = 0.83$ for $Al_xGa_{1-x}N$ LEDs. This result appears to indicate that the light-polarization switching behavior might not be that important in deep UV AlGaN emitters. At the moment, there is neither clarity nor consensus on the subject. However, a lot of scattered data is available in the literature. These data appear to indicate that the critical Al composition at which the emitted light switches its polarization characteristics varies from $x = 0.125$ to $x = 0.83$.[2,3,8,10,13,14] In this article, we discuss the fundamental physics related to the anticrossing of the valence bands and to the polarization switching of light emitted from $Al_xGa_{1-x}N$ epilayers. A quantitative analysis of the experimental data is essential for gaining a clear understanding of the switching of polarization characteristics of light emitted from $Al_xGa_{1-x}N$ epilayers.

II. NUMERICAL MODELING AND SIMULATIONS

In our analysis, the modification of the electronic band structure and hole effective mass due to strain was taken into account using a 6 × 6 k.p formalism based on the Bir–Pikus Hamiltonian. This approach is now widely accepted in the nitride community.[13,15–19] All the materials parameters used in our calculations were taken from the literature.[19–21] The

 ©2011 American Physical Society

required parameters for the ternary alloys were interpolated by using appropriate values of the relevant binary GaN and AlN nitride materials. We then carried out meticulous quantum mechanical calculations aimed at estimating the ground state emission wavelength of wurtzite $Al_xGa_{1-x}N/Al_zGa_{1-z}N$ ($x < z$) QW structures suitable for active regions of deep UV emitters. We numerically solve the Schrödinger equation for finite, square potential wells in the conduction and valence bands using the envelope function approximation. At the Brillouin zone center (the Γ-point), the conduction band (CB) of AlGaN is composed of atomic s-orbitals with wave functions of $|S\rangle$ symmetry, whereas the three uppermost valence bands (VBs) are made up of p-orbitals with the wave functions being a combination of $|X\rangle$, $|Y\rangle$, and $|Z\rangle$ symmetry. A downward transition involving electrons in an $|S\rangle$-like CB state and holes in an $|X\rangle$-like, $|Y\rangle$-like, or $|Z\rangle$-like VB state would emit light polarized along the x, y, or z Cartesian directions, respectively. Here, the c-axis of the AlGaN wurtzite crystal is assumed to be parallel to the z-axis of the Cartesian system. We adopt a nomenclature wherein the strain-modified excitonic transitions are labeled T_1, T_2, and T_3 in order of increasing energy. Their polarization properties are determined by the relative oscillator strength components f_{ij}, with $i = 1, 2, 3$ and $j =$ x, y, z, representing the three transitions and their polarization components, respectively. The values of the matrix elements $|\langle S|p_x|X\rangle|^2$, $|\langle S|p_y|Y\rangle|^2$, and $|\langle S|p_z|Z\rangle|^2$ in AlGaN are expected to be nearly equal, leading to the following oscillator strength sum rules: $\sum_{i=1}^{3} f_{i,j} = 1$ and $\sum_{j=x}^{z} f_{i,j} = 1$.[16,19]

III. RESULTS AND DISCUSSION

Because of the negative value of the crystal field splitting in AlN, the valence bands are expected to switch their position at some critical Al composition in the $Al_xGa_{1-x}N$ layers.[2,14] However, nitride epilayers grown on foreign substrates such as sapphire or SiC have a tendency to possess some residual strain.[19,20,31] The critical Al composition in the $Al_xGa_{1-x}N$ layers therefore depends on the magnitude of the residual strain, as indicated by Ikida *et al.*[14] Using a qualitative model for the strain dependence of the crystal field splitting, Banal *et al.*[2] predicted that the bands should switch character at $x = 0.60$ for $Al_xGa_{1-x}N$ layers grown on unstrained AlN. However, they observed switching of the light-polarization characteristics at $x \sim 0.80$, which was explained by assuming the presence of some residual compressive strain in the AlN templates. If this is true, then $Al_xGa_{1-x}N$ ($x > 0.60$) QWs grown on strain-free AlN templates or substrates might not be suitable for developing efficient deep UV LEDs with TE-mode characteristics. However, this contradicts recent observations by Hirayama *et al.*,[3] who reported vertical emission of light (out of the c-plane) for aluminum compositions up to $x = 0.83$. It should be noted that LED structures in the deep UV range are not usually grown on GaN or AlN, but on Al-rich $Al_xGa_{1-x}N$ templates or buffer layers to accommodate strain-free, thick barrier layers.[3–5,7] It is therefore important to raise the question of what the critical aluminum composition is at which the two valence bands switch their character for $Al_xGa_{1-x}N$ layers grown on an $Al_yGa_{1-y}N$ template ($x < y$). With this in mind, we have carried out detailed theoretical calculations

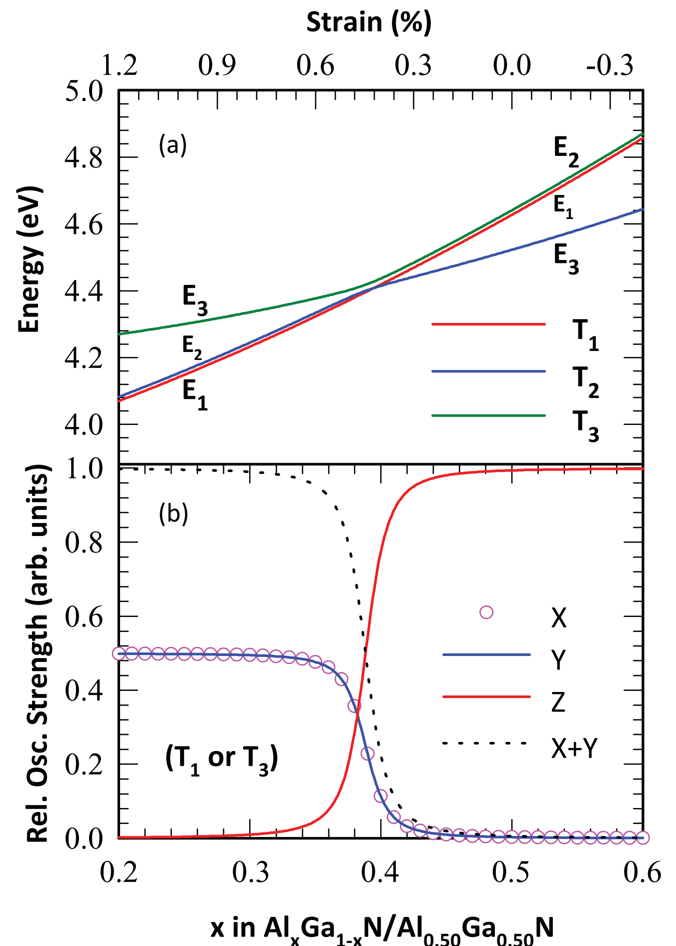

FIG. 1. (Color online) (a) Excitonic band gaps E_1, E_2, and E_3 corresponding to the three valence bands VB_1, VB_2, and VB_3 and (b) relative oscillator strength of the lowest excitonic transition (T_1 or T_3) under strain for light polarized along the x, y, and z directions, plotted as functions of composition (bottom axis)/residual strain (top axis), respectively, for $Al_xGa_{1-x}N$ layers grown on $Al_{0.50}Ga_{0.50}N$ templates. Note the anticrossing of the band gaps at $x \sim 0.4$, corresponding to the strain-induced switching of the character of the valence bands.

as described earlier and a typical example of the results is shown in Fig. 1(a). Here, we plot the band gaps E_1, E_2, and E_3 at the Γ-point corresponding to the three valence bands VB_1, VB_2, and VB_3 of an $Al_xGa_{1-x}N$ ternary alloy grown on $Al_{0.50}Ga_{0.50}N$ free-standing substrate or template as a function of aluminum mole fraction x or equivalent strain. One notes that the two uppermost valence bands remain more or less degenerate (corresponding to $E_2 - E_1 < 15$ meV) for $x \leqslant \sim 0.40$; whereas, for $x > 0.40$, the degeneracy is lifted, and the band gap E_3 becomes the smallest one. Well below the lattice-matching composition, there is an anticrossing of the bands, even for compressive strain in the $Al_xGa_{1-x}N$ alloy; the two valence bands corresponding to E_2 and E_3 essentially switch their character.

Another important consequence of the strain-induced band structure modifications in Al-rich AlGaN QWs is a strong preference for TM polarization of the emitted light. We summarize the essential features of the effect on polarization

in Fig. 1(b), where we plot the relative oscillator strength of the lowest excitonic transition (T_1 or T_3, depending on which band gap, E_1 or E_3, is lower) under strain for light polarized along the x, y, and z direction for the $Al_xGa_{1-x}N$ layer. For purposes of comparison, we also show the additive values of the relative oscillator strength for the two components of polarization; in this case $(X + Y)$, which determine the maximum fraction of light traveling perpendicular to the c-plane, for example, in LEDs grown on c-plane sapphire. For aluminum compositions of $x > 0.40$ in an $Al_xGa_{1-x}N$ QW, one notes that a good fraction of the emitted light is polarized along the c-axis (as represented by the relative oscillator strength along the z-axis). This is highly inconvenient for light extraction from LEDs whose output is expected along the c-axis. It is a fact that high Al-content in the active regions of LEDs is desirable for light emission at short wavelengths. However, inappropriate structural designs can lead to highly inefficient devices due to strain-induced light-polarization switching effects. These effects are often not properly accounted for in the design of LED devices. This situation is further complicated by the presence of a thick barrier or buffer layers whose lattice constants are vastly different from that of the template or substrate. The barrier or buffer layers are bound to have some residual strain that alters the band structure of epilayers grown on top of them. In view of this, we plot the numerically calculated polarization switching characteristics of $Al_xGa_{1-x}N$ layers that are assumed to be grown on $Al_yGa_{1-y}N$ templates (for $x < y$) in Fig. 2. The interpolated values of the crystal field splitting energy for the $Al_xGa_{1-x}N$ alloy are also plotted on the same graph (right axis). For $x \approx 0.04$, the crystal field splitting changes its sign, indicating a possible switching of polarization characteristics. However, the critical Al composition increases because of residual strain in the $Al_xGa_{1-x}N$ layers, as indicated in Fig. 2. The polarization characteristics are expected to switch at $x \approx 0.80$ for $Al_xGa_{1-x}N$ layers grown on free-standing AlN (where $y = 1$) templates or substrates. This supports the observations of Banal *et al.*,[2] who reported polarization switching at $x \approx 0.80$ for $Al_xGa_{1-x}N$/AlN QW structures. In Fig. 3, we plot the critical Al composition in $Al_xGa_{1-x}N$ layers that leads to polarization switching in such layers if these were grown on free-standing $Al_yGa_{1-y}N$ templates or substrates of certain aluminum composition, y. The curve for 50% (1%) oscillator strength (Osc) represents the critical Al composition to ensure that 50% (1%) of the generated light travels parallel to the c-axis. The curve for Osc = 1% indicates that the emitted light is strongly TM-polarized. These calculations clearly show that the critical Al composition increases linearly with the Al content in the $Al_yGa_{1-y}N$ templates or substrates. For comparison purposes, we have also plotted the calculated values of the critical Al composition obtained using the qualitative model from Ref. 2. The qualitative model appears to be reasonable for Al-rich $Al_yGa_{1-y}N$ templates ($y > 0.90$); however, it overestimates the critical Al composition for $Al_xGa_{1-x}N$ layers grown on $Al_yGa_{1-y}N$ templates with $y < 0.90$. Recently, the effect of the crossover of valence bands on gain characteristics of high–Al-content $Al_xGa_{1-x}N$ QW lasers have been discussed by Zhang *et al.*,[22] where they predicted a band crossover at $x = 0.572$. However, they did not discuss the dependence of valence band crossover in $Al_xGa_{1-x}N$ layers on the composition of template or buffer.

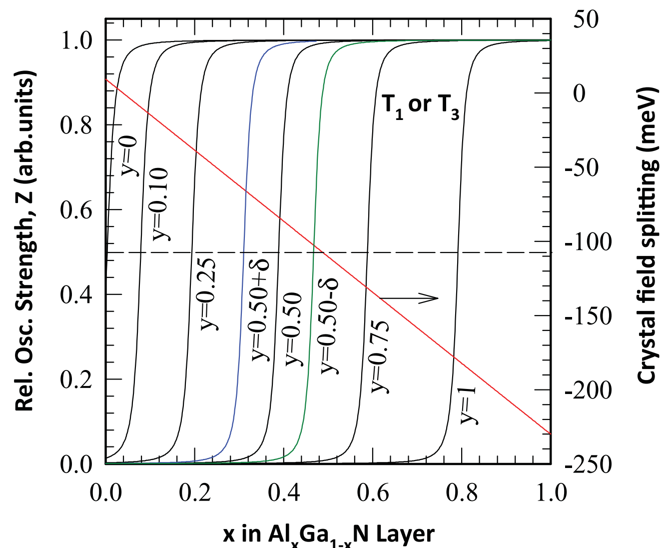

FIG. 2. (Color online) Relative oscillator strength of the lowest excitonic transition (T_1 or T_3) under strain for light polarized along the z direction plotted as functions of Al compositions of $Al_xGa_{1-x}N$ layers grown on $Al_yGa_{1-y}N$ templates. Switching of the light polarization from TE to TM mode occurs whenever the oscillator strength increases >0.5, as shown by a dashed line that defines the critical Al composition of $Al_xGa_{1-x}N$ layers grown on $Al_yGa_{1-y}N$ templates. The effect of residual strain ($\delta = 0.4\%$) in $Al_{0.50}Ga_{0.50}N$ templates on the corresponding critical Al composition of $Al_xGa_{1-x}N$ layers is also shown. The interpolated values of the crystal field splitting of the $Al_xGa_{1-x}N$ layers are shown in the same graph (right axis).

It is interesting to compare and discuss the observations of Banal *et al.*[2] and Hirayama *et al.*,[3] which we present in Table I. According to the experimental results of Banal *et al.*,[2] the critical Al composition for $Al_xGa_{1-x}N$ QW structures grown on AlN templates is ≈0.80; this value is in good agreement with our theoretical prediction as discussed here. Using a qualitative model, Banal *et al.*[2] predict that the polarization should switch from TM to TE for an $Al_xGa_{1-x}N$ QW structure with $x = 0.82$ because of quantum confinement effects if the QW thickness is kept <3 nm. Using data from our model, we plot the energy values of ground state transitions corresponding to the three valence bands of an $Al_{0.82}Ga_{0.18}N$/AlN QW structure in Fig. 4. The calculations indicate that the emitted light would be TM-polarized (where the T_3 transition is the lowest) for QW thicknesses >5 nm. However, the polarization should switch to the TE mode (when the T_1 transition becomes the lowest) for QW thicknesses <5 nm. Contrary to the qualitative model,[2] we find that the band gap E_3, corresponding to the valence band VB_3 never becomes the largest of the three because of quantum confinement effects.

The experimental results of Hirayama *et al.*[3] shown in Table I are similarly in agreement to our calculations, except for the sample with $x = 0.83$, where theory predicts TM-polarized light. For this particular QW sample, the valence bands switch their positions at a QW thickness of 2 nm because of quantum confinement effects. This leads to TE-polarized light. We note that the QW thicknesses used by Hirayama *et al.*,[3–5,7] are <2 nm, confirming our predictions. We point

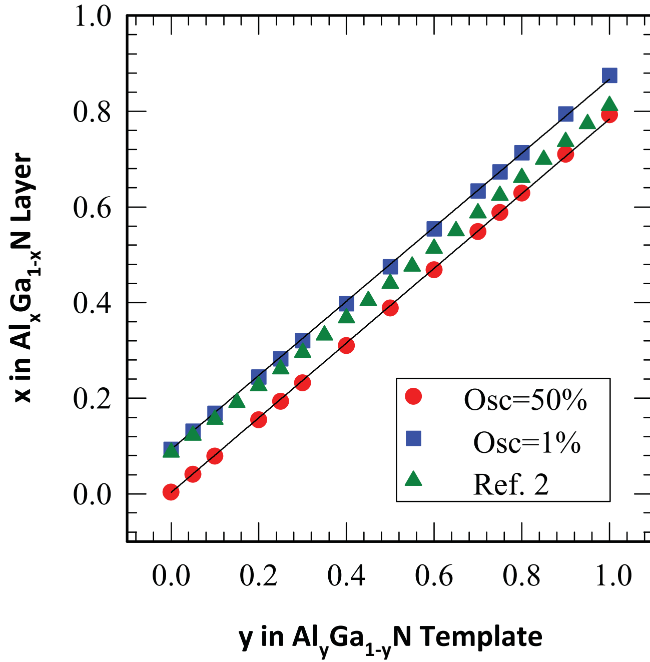

FIG. 3. (Color online) The critical Al composition in $Al_xGa_{1-x}N$ layers leading to a switching of the light-polarization characteristics (Osc = 50%) plotted as a function of composition of the $Al_yGa_{1-y}N$ templates. For comparison, values of critical Al compositions obtained from a qualitative model[2] and the Al composition that supports strongly TM-polarized light (Osc = 1%) emission are also shown in the same graph.

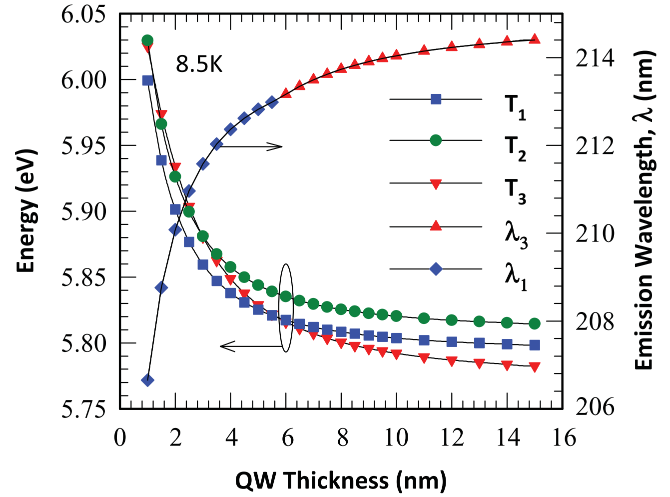

FIG. 4. (Color online) Ground state energies of the T_1, T_2, and T_3 excitonic transitions in an $Al_{0.82}Ga_{0.18}N$/AlN QW structure corresponding to the three band gaps E_1, E_2, and E_3, plotted as a function of QW thickness. The emission wavelength corresponding to the lowest excitonic transition is also indicated on the same graph (right axis). The wavelengths of TM- and TE-polarized emitted light are indicated by λ_3 and λ_1; these correspond to the T_3 and T_1 excitonic transitions, respectively; note the switching position at a QW thickness of 5 nm.

out that most deep UV LED structures are often grown on thick $Al_yGa_{1-y}N$ barrier or buffer layers that might be partially or fully relaxed. Any such relaxation processes would further influence the polarization characteristics of the emitted light. This is indicated in Fig. 2, where two additional curves for $y = 0.5$ (with $y = 0.5 \pm \delta$) are plotted to include the residual strain (δ) in the $Al_yGa_{1-y}N$ barrier or buffer layer. Therefore, if a thick relaxed $Al_yGa_{1-y}N$ buffer layer with $y = 0.84$ is used in an LED structure, the emitted light from an $Al_xGa_{1-x}N$ QW with $x = 0.67$ should be TM-polarized, as observed by Kawanishi *et al.*[10] In contrast, the emission characteristics of LEDs made by Hirayama *et al.*[3] turn out to be TM-polarized for two of their samples when the buffer layers are assumed to be relaxed. Even with quantum confinement effects, the polarization cannot be switched back to the TE mode. Furthermore, these devices were reported to have very low EQE values. It is important to note that the angular dependence of the light emanating from the LEDs reported by Hirayama *et al.*[3] only represents the light fraction that is accommodated in the escape cone, which is not necessarily a good measure for polarization characteristics of light emitted by a QW structure.

In the foregoing treatment and discussion, we have ignored the effects of polarization-induced electric fields for simplicity; these are known to lead to a red shift in the emission wavelength and a reduction in device efficiency because of the separation of the electron and hole wave functions. In shallow wells, the polarization-induced electric field can facilitate thermal ejection of charge carriers from the QWs. However, these effects can be reasonably suppressed under heavy current injection conditions for very thin QWs (<2 nm), such as those

TABLE I. Experimental and theoretical light-polarization characteristics of $Al_xGa_{1-x}N$ QW structures grown on $Al_yGa_{1-y}N$ buffer or barrier layers on AlN/sapphire templates. The acronyms TE and TM stand for the transverse electric and transverse magnetic light polarizations, respectively.

Reference	Template/ substrate	y in $Al_yGa_{1-y}N$ barrier/buffer layer	x in $Al_xGa_{1-x}N$ quantum well	Polarization experiment (TE/TM)	Polarization theory (TE/TM)
2	AlN/sapphire	1	0.69	TE	TE
		1	0.82	TE/TM[a]	TE/TM[a]
		1	0.91	TM	TM
3	AlN/sapphire	0.89	0.83	TE	TE/TM[a]
		0.84	0.74	TE	TE
		0.76	0.61	TE	TE

[a]Quantum confinement changes the polarization of emitted light from TM to TE mode.

common in deep-UV nitride emitters. These effects are known to be less prominent for AlGaN QWs emitting in the UV range compared with InGaN QWs emitting in the blue-green spectral region.[23–25] From a qualitative model, it has also been predicted that the critical Al composition remains largely unaffected by the polarization-induced electric field for thin QWs.[2] To be a little more cautious, it is important to estimate the effect of the polarization-induced internal electric fields on the critical Al composition within the framework of the proposed numerical model.

In our calculations, the magnitude of the internal electric field in the AlGaN QW and AlN barrier layers was estimated using a well-established numerical model.[26–29] The material parameters for these calculations were taken from the published literature.[19–21,27] It was assumed that the AlN barrier layers are fully relaxed and that the AlGaN QW layer is compressively strained. The AlN barrier layers would therefore have the electric field induced only by spontaneous polarization, whereas the AlGaN QW layer might posses an electric field induced by both spontaneous as well as piezoelectric polarization. The magnitude of the internal electric field in the AlN barrier layer and the $Al_{0.82}Ga_{0.18}N$ QW layers was calculated to be $F_b = -165$ kV/cm and $F_{qw} = 551$ kV/cm, respectively, as shown in Fig. 5. This figure illustrates an example of the Schrödinger equation solution for electrons confined in the CB potential well for three QW thicknesses under the influence of internal electric fields. The relative occupation probability density for electrons in the respective CB is also plotted on the same graph, where $P_f = |\psi_f|^2$ and $P_o = |\psi_o|^2$ represent the calculated occupation probability density for electrons; ψ_f and ψ_o are the electron wave functions, with and without electric fields, respectively. A reduction in the electron energy eigenvalues and localization of the electrons near the tip of the triangular-shaped potential well is clearly evident; the former effect leads to the well-known red shift in the emission wavelength, whereas the latter, the separation of the electron and hole wave functions, leads to reduced emission efficiency because of the reduced wave function overlap.

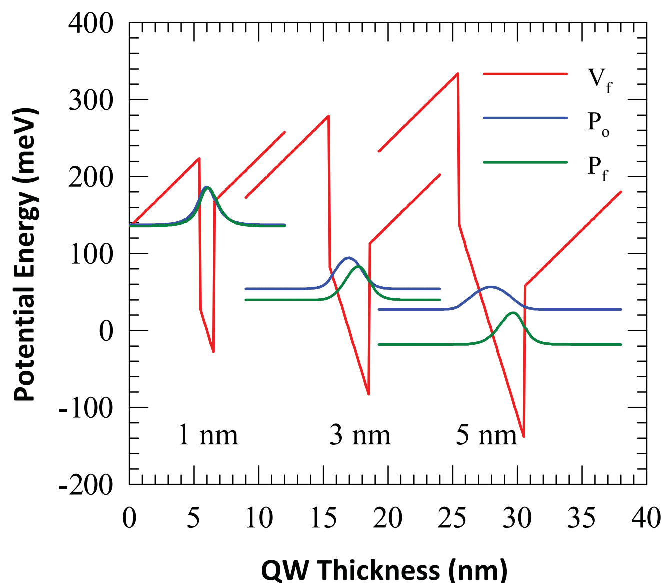

FIG. 5. (Color online) Conduction band potential well (V_f) profiles of three $Al_{0.82}Ga_{0.18}N$/AlN QW structures of different well widths under the influence of polarization-induced electric fields ($F_b = -165$ kV/cm, $F_{qw} = 551$ kV/cm). The relative occupation probability density of electrons in the respective CB is also plotted in the same figure, where $P_f = |\psi_f|^2$ and $P_o = |\psi_o|^2$ represent the calculated occupation probability densities for electrons; ψ_f and ψ_o are the electron wave functions with and without electric field, respectively.

The influence of internal electric fields on the critical Al composition in QWs can be understood from Fig. 6(a), where we plot the energy values of the ground state transitions corresponding to the three valence bands of an $Al_{0.82}Ga_{0.18}N$/AlN QW structure (as an example) by taking into account the polarization-induced electric fields. These calculations indicate that the emitted light would be TE-polarized, irrespective of the QW thickness, where no valence band switching is expected. In contrast to the data presented in Fig. 4 for the same QW structure where internal electric fields were ignored, we find that the critical QW thickness for valence band switching depends on the magnitude of the internal electric field. It is possible that the internal electric field might be screened by several other effects, where flat band conditions might be achieved under heavy current injection in LEDs and LDs. In the $Al_{0.82}Ga_{0.18}N$/AlN QW structure, polarization-induced electric fields seem to play an important role, as illustrated in Fig. 6(b), where the emission wavelength is plotted as a function of QW thickness with and without polarization-induced electric fields. This figure suggests that the red shift induced by the internal electric field in the $Al_{0.82}Ga_{0.18}N$/AlN QW should be minimal (<3 nm) for thin QWs (<4 nm)—which is in good agreement with experimental results.[23] The separation between the two uppermost valence bands in the $Al_{0.82}Ga_{0.18}N$ QW is plotted in Fig. 6(c); for this particular structure, switching of the position for the two valence bands is expected in the absence of internal electric fields. However, no band switching is expected under the influence of internal electric fields for this QW structure. The polarization properties of light emitted by an $Al_{0.82}Ga_{0.18}N$/AlN QW therefore depend on QW thickness and possible screening of the polarization-induced electric fields.

We now want to understand the effect of polarization-induced electric fields on the emission properties of $Al_{0.91}Ga_{0.09}N$/AlN QWs, where TM-polarized light emission has been observed in reported experiments,[2] and supported by the theoretical predictions summarized in Table I. In Fig. 7(a) and 7(b), we plot the energy values of the ground state transitions corresponding to the three valence bands of the $Al_{0.91}Ga_{0.09}N$/AlN QW structure without and with the polarization-induced electric fields. The calculated magnitude of the internal electric field in the AlN barrier and $Al_{0.91}Ga_{0.09}N$/AlN QW layers is $F_b = -83$ kV/cm and $F_{qw} = 277$ kV/cm, respectively. In Fig. 7(c), we plot the transition energies for the $Al_{0.91}Ga_{0.09}N$/AlN QW structure discussed earlier, but with much larger magnitudes for the internal electric fields. This value of the internal electric field is taken from the $Al_{0.82}Ga_{0.18}N$/AlN QW structure shown in Fig. 6(a). Even though the three valence bands are expected to lie a little closer, no band switching is observed at larger magnitudes of the internal electric fields. These calculations indicate that light emitted from an $Al_{0.91}Ga_{0.09}N$/AlN QW

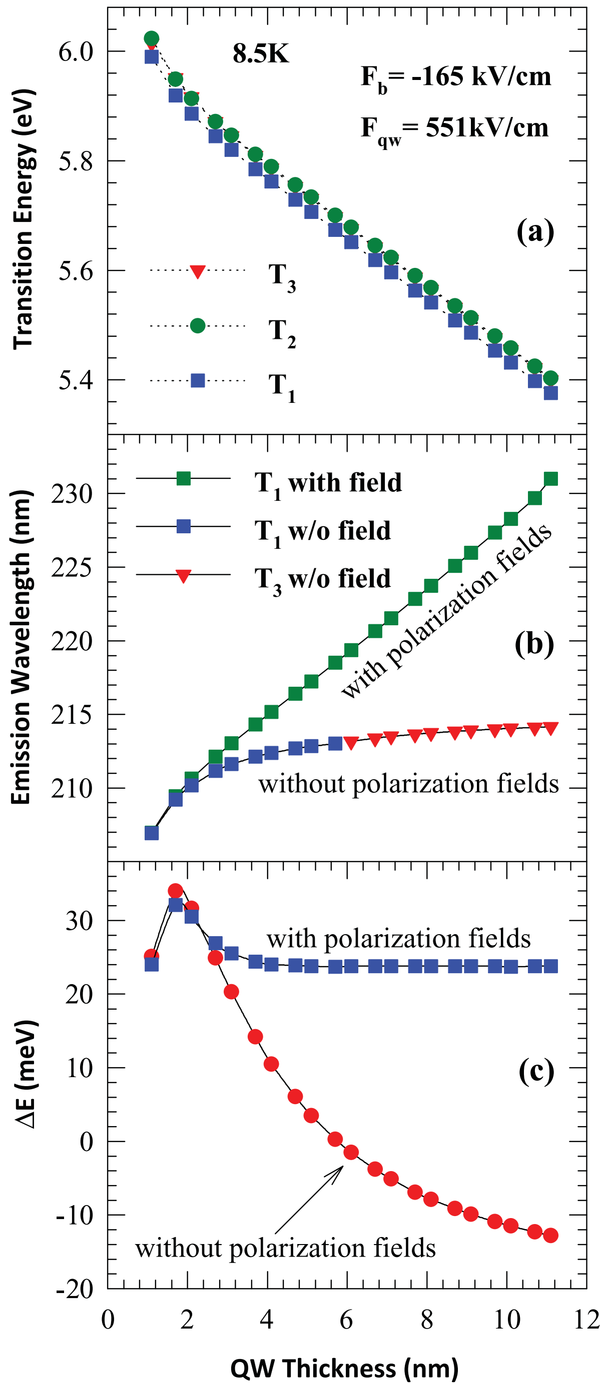

FIG. 6. (Color online) (a) Ground state energies of the T_1, T_2, and T_3 excitonic transitions of an $Al_{0.82}Ga_{0.18}N$/AlN QW structure corresponding to the three band gaps of E_1, E_2, and E_3 under the influence of polarization-induced electric fields, (b) the emission wavelength corresponding to the lowest excitonic transition with and without electric field, and (c) the separation between the two topmost valence bands of the $Al_{0.82}Ga_{0.18}N$ QW plotted as a function of QW thickness.

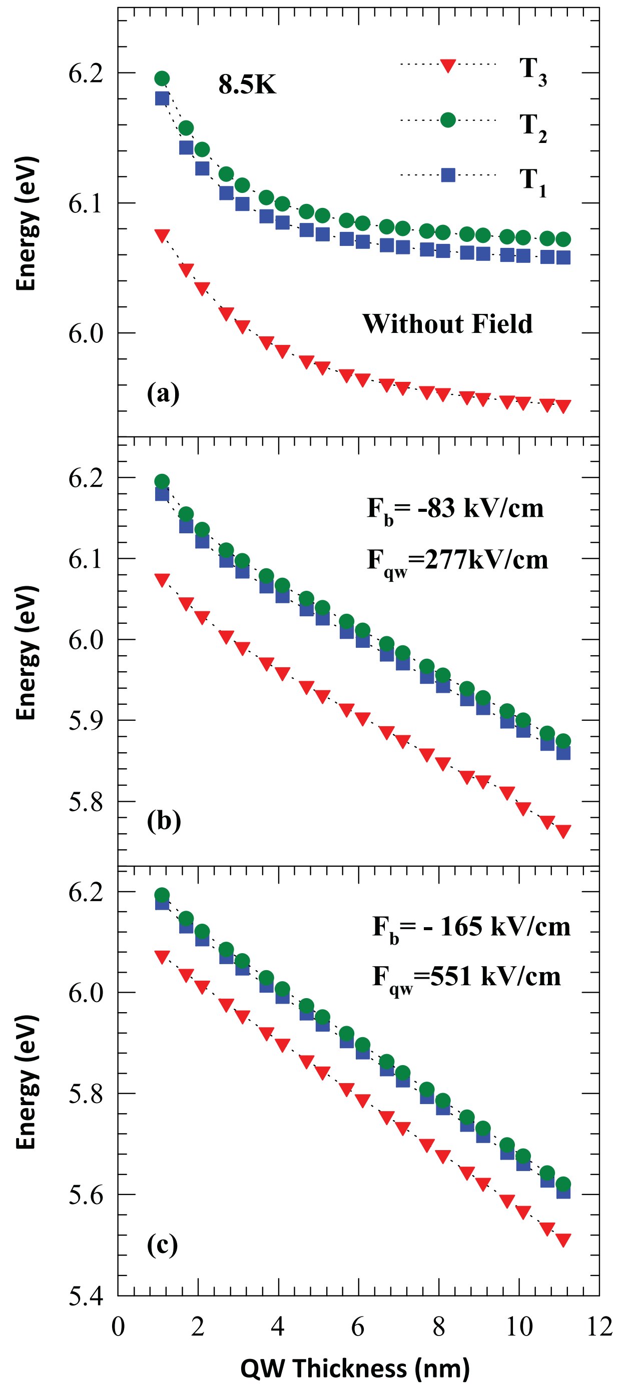

FIG. 7. (Color online) (a) Ground state energies of the T_1, T_2, and T_3 excitonic transitions in an $Al_{0.91}Ga_{0.09}N$/AlN QW structure corresponding to the three band gaps of E_1, E_2, and E_3 with polarization-induced electric fields neglected, (b) with polarization-induced electric fields included, and (c) with large polarization-induced electric field that is taken from $Al_{0.82}Ga_{0.18}N$/AlN QW structure, plotted as a function of QW thickness.

structure should be TM-polarized, irrespective of the QW thickness or magnitude of the internal electric fields.

We find therefore that polarization-induced electric fields do not lead to switching of valence band positions if the Al-composition in the QW is kept below or higher than the critical Al composition. It is only in special cases, such as that of the $Al_{0.82}Ga_{0.18}N$ QW structure in Ref. 2, where the three valence bands lie in close proximity, that this can happen; it is brought about by either the QW thickness or polarization-induced electric fields. In all other cases, the polarization properties of the emitted light are determined by the residual strain in

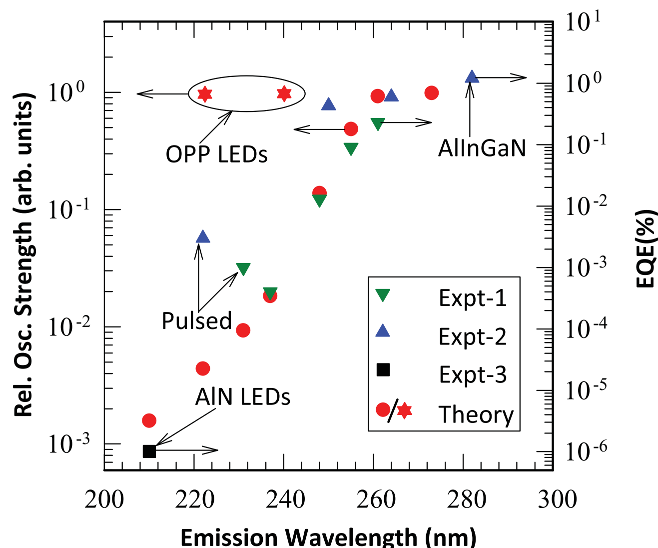

FIG. 8. (Color online) Relative oscillator strength for the lowest excitonic transition (T_1 or T_3) for AlGaN QWs plotted as a function of emission wavelength. For comparison, values of the external quantum efficiencies (EQE) are also plotted on the same graph (Exp. 1, Ref. 3; Exp. 2, Ref. 7; Exp. 3, Ref. 30). The relative oscillator strengths for optimized polarization properties (OPP) of two LED structures designed for TE-mode emission are also indicated (with stars). EQE values <240 nm are for the LEDs that were operated under pulse conditions.

the QW layer; this has an associated critical Al composition dictated by the choice of the substrate/template. It is therefore important to keep these facts in mind during the design process of deep UV light emitters based on AlGaN epitaxial layers.

Finally, we plot the calculated values of the relative oscillator strength for the lowest excitonic transition (T_1 or T_3) for $Al_xGa_{1-x}N/Al_zGa_{1-z}N$ QWs grown on $Al_yGa_{1-y}N$ ($x < z < y$) templates as functions of the emission wavelength in Fig. 8. The values of the Al compositions (x, y, and z) for different QW structures were taken from those corresponding to LED structures in the literature (Exp. 1, Ref. 3; Exp. 2, Ref. 7; Exp. 3, Ref. 30). Note that the calculated values of the relative oscillator strength for the lowest excitonic transition decrease rapidly as the wavelength of 200 nm is approached for Al-rich AlGaN QWs. For comparison, the experimentally measured values of the EQE, taken from the same references, are also plotted on the same graph (right axis).[3,7,30] In addition, we have included reported EQE values for AlInGaN and AlN LEDs as benchmarks. This figure illustrates that reduction of the oscillator strength as the wavelength becomes shorter in $Al_xGa_{1-x}N$ QWs tracks the decrease in EQE values. This correlation reasonably explains the drop in EQE values usually observed in the deep UV LEDs. It is related to the dominance of TM-polarized light that is difficult to extract from LEDs grown on c-plane templates or substrates. This issue has not been properly addressed in deep UV LEDs, where the precipitous decrease in EQE is usually blamed on problems in epitaxial growth, such as difficulties in achieving high electrical conductivity in p-type AlGaN barrier layers.[3–5,7] Theoretical calculations predict that the EQE of AlN homojunction LEDs should be lower by about three orders of magnitude compared with the AlGaN LEDs operating at 280 nm, even when problems in epitaxial growth are resolved. To develop efficient deep UV LEDs, it is therefore essential to design the QW structures with compressive residual strain by choosing suitable $Al_yGa_{1-y}N$ templates or buffers that ensure TE-polarized light emission. One optimal LED design for TE-polarized light emission at ∼240 nm, for example, might include an $Al_{0.62}Ga_{0.38}N/Al_{0.80}Ga_{0.20}N$ QW structure in the active region grown on $Al_{0.85}Ga_{0.15}N$ template or substrate. For TE-mode emission at the shorter wavelength of 220 nm, the QW could be composed of an $Al_{0.75}Ga_{0.25}N/Al_{0.90}Ga_{0.10}N$ QW structure grown on an AlN template or substrate. The values of the relative oscillator strength, as figures of merit, for these two LED structures with optimized polarization properties (OPP) are indicated (with stars) in Fig. 8. Light emission for these proposed LED structures would be TE-polarized, even under the influence of polarization-induced electric fields.

IV. SUMMARY AND OUTLOOK

In summary, we find a linear relationship between the critical Al compositions in $Al_xGa_{1-x}N$ epilayers used in active region of LEDs and the Al fraction in associated $Al_yGa_{1-y}N$ templates or substrates. The polarization characteristics of light emitted from such active layers switch from TE to TM mode at some critical Al compositions. The critical Al composition in the active layer depends on the amount of residual strain in the $Al_yGa_{1-y}N$ templates or substrates used. An accurate quantitative estimate of the strain-driven critical Al composition in the $Al_xGa_{1-x}N$ layers is indispensible, especially when quantum confinement effects play a critical role in determining the emission characteristics of the QW structures. Because strain-induced light-polarization switching can lead to a reduction in light extraction efficiency for LEDs, it is imperative to determine *a priori* what the optimal device design parameters should be. We suggest two possible QW structures designed to emit TE-polarized light in the deep UV. These structures have the potential to achieve EQE values comparable to those reported in 280-nm LEDs. We note that although higher Al content in AlGaN QWs might lead to shorter emission wavelengths (<220 nm), this comes at a price that includes poor carrier confinement, lower extraction of TM-polarized light, and higher threshold current densities. Furthermore, it is of paramount importance to assure that the Al-rich p-type AlGaN barrier layers are doped to the highest level possible (without deleterious effects) to guarantee optimal hole injection into the active region. Finally, the phenomenon of the critical Al composition that causes light-polarization switching in AlGaN-based ultraviolet light emitters is of a fundamental nature. It must be taken into consideration in the design process of deep UV emitters.

ACKNOWLEDGMENTS

The authors acknowledge partial financial support from the US Defense Advanced Research Projects Agency through the US Air Force at Hanscom Air Force Base in Bedford, MA, for their work on nitride semiconductors (Grant No. FA-871808-c-0035). T.K.S. thanks Sandip Ghosh and S. D. Singh for assistance with the computations and for useful discussions.

[*]Corresponding author: tarun@rrcat.gov.in
[†]Present address: Semiconductor Laser Section, Raja Ramanna Centre for Advanced Technology, Indore 452 013 (M.P.), India.
[‡]towe@cmu.edu

[1]T. Oto, R. G. Banal, K. Kotaoka, M. Funato, and Y. Kawakami, Nature Photon. doi:10.1038/nphoton.2010.220 (2010).
[2]R. G. Banal, M. Funato, and Y. Kawakami, Phy. Rev. B **79**, 121308R (2009).
[3]H. Hirayama, N. Noguchi, and N. Kamata, Appl. Phys. Express **3**, 032102 (2010).
[4]H. Hirayama, Y. Tsukada, T. Maeda, and N. Kamata, Appl. Phys. Express **3**, 031002 (2010).
[5]H. Hirayama, T. Yatabe, N. Noguchi, T. Ohashi, and N. Kamata, Electron. Commun. Jpn. **93**, 748 (2010).
[6]W. Sun, M. Shatalov, J. Deng, X. Hu, J. Yang, A. Lunev, Y. Bilenko, M. Shur, and R. Gaska, Appl. Phys. Lett. **96**, 061102 (2010).
[7]H. Hirayama, S. Fujikawa, N. Noguchi, J. Norimatsu, T. Ta-kano, K. Tsubaki, and N. Kamata, Phys. Status Solidi A **206**, 1176 (2009).
[8]K. B. Nam, J. Li, M. L. Nakarmi, J. Y. Lin, and H. X. Jianga, Appl. Phys. Lett. **84**, 5264 (2004).
[9]H. Kawanishi, M. Senuma, M. Yamamoto, E. Niikura, and T. Nukui, Appl. Phys. Lett. **89**, 081121 (2006).
[10]H. Kawanishi, M. Senuma, and T. Nukui, Appl. Phys. Lett. **89**, 041126 (2006).
[11]J. Shakya, K. H. Kim, J. Y. Lin, and H. X. Jiang, Appl. Phys. Lett. **85**, 142 (2004).
[12]J. Shakya, K. Onabe, K. H. Kim, J. Li, J. Y. Lin, and H. X. Jiang, Appl. Phys. Lett. **86**, 091107 (2005).
[13]K. Hazu, T. Hoshi, M. Kagaya, T. Onuma, and S. F. Chichibu, J. Appl. Phys. **107**, 033701 (2010).
[14]H. Ikeda, T. Okamura, K. Matsukawa, T. Sota, M. Sugawara, T. Hoshi, P. Cantu, R. Sharma, J. F. Kaeding, S. Keller, U. K. Mishra, K. Kosaka, K. Asai, S. Sumiya, T. Shibata, M. Tanaka, J. S. Speck, S. P. DenBaars, S. Nakamura, T. Koyama, T. Onuma, and S. F. Chichibu, J. Appl. Phys. **103**, 089901 (2008).
[15]M. Suzuki, T. Uenoyama, and A. Yanase, Phy. Rev. B **52**, 8132 (1995).
[16]M. Suzuki and T. Uenoyama, Jpn. J. Appl. Phys. **35**, 543 (1996).
[17]A. Shikanai, T. Azuhata, T. Sota, S. Chichibu, A. Kuramata, K. Horino, and S. Nakamura, J. Appl. Phys. **81**, 417 (1997).
[18]S. Ghosh, P. Waltereit, O. Brandt, H. T. Grahn, and K. H. Ploog, Phy. Rev. B **65**, 075202 (2002).
[19]J. Bhattacharyya, S. Ghosh, and H. T. Grahn, Phys. Status Solidi B **246**, 1184 (2009).
[20]I. Vurgaftman and J. R. Meyer, J. Appl. Phys. **94**, 3675 (2003).
[21]P. Rinke, M. Winkelnkemper, A. Qteish, D. Bimberg, J. Neugebauer, and M. Scheffler, Phy. Rev. B **77**, 075202 (2008).
[22]J. Zhang, H. Zhao, and N. Tansu, Appl. Phys. Lett. **97**, 111105 (2010).
[23]H. Yoshida, Y. Yamashita, M. Kuwabara, and H. Kan, Nature Photon. **2**, 551 (2008).
[24]D. F. Feezell, M. C. Schmidt, S. P. DenBarrs, and S. Nakamura, MRS Bull. **34**, 318 (2009).
[25]K. Kazlauskas, G. Tamulaitis, J. Mickevièius, E. Kuokštis, A. Žukauskas, Y. C. Cheng, H. C. Wang, C. F. Huang, and C. C. Yang, J. Appl. Phys. **97**, 013525 (2005).
[26]S. H. Park and S. L. Chuang, Appl. Phys. Lett. **76**, 1981 (2000).
[27]S. H. Park and S. L. Chuang, J. Appl. Phys. **87**, 353 (2000).
[28]A. Bykhovski, B. Gelmont, and M. Shur, J. Appl. Phys. **74**, 6734 (1993).
[29]V. Fiorentini, F. Bernardini, F. D. Sala, A. D. Carlo, and P. Lugli, Phy. Rev. B **60**, 8849 (1999).
[30]Y. Taniyasu, Makoto Kasu, and T. Makimoto, Nature **441**, 325 (2006).
[31]Updated values of deformation potentials for AlN, crystal field splittings and bandgaps have been taken from Refs. 19 and 21.